Fractional Wave Propagation in Asymmetric Nonlinear Media: Implications for Metamaterial-Based Wave Control

Maryam Sabzevar [a] , **Mohammad Hossein Ehsani** [a*] , **Mehdi Solaimani** [b]

[a] *Faculty of Physics, Semnan University, Semnan 35195-363, Iran*

[b] *Department of Physics, Qom University of Technology, Qom 1519-37195, Iran*

A R T I C L E   I N F O

A B S T R A C T

This study investigates the phenomenon of superarrival in Gaussian wave packets propagating through a nonlinear fractional medium under the influence of a triangular potential barrier. The time-dependent fractional Schrödinger equation is numerically solved using the Split-Step Finite Difference method to analyze the wave packet dynamics and transmission behavior in detail. The magnitude of superarrival is quantified and examined across a broad range of physical parameters, including the fractional order, nonlinearity strength, dispersion coefficient, wave packet width, initial velocity, and potential asymmetry. Results reveal that superarrival is significantly enhanced in fractional and weakly nonlinear regimes and is highly sensitive to the degree of potential asymmetry. The observed behavior reflects the interplay between nonlocality and nonlinearity, characteristic of complex and engineered materials. These insights contribute to a deeper understanding of early arrival phenomena in wave dynamics and may provide theoretical support for controlling energy or information transport in next-generation devices. Potential applications include quantum control, signal processing in photonic systems, and the design of metamaterials with tailored transmission properties at ultrafast or subwavelength scales.

1. Introduction

Fractional calculus is a branch of mathematical analysis concerned with integrals and derivatives of arbitrary (non-integer) order. This intriguing field has found extensive applications in modeling complex physical systems and processes where traditional calculus falls short. Various fractional differential equations have emerged, including the fractional wave equations for compressional and shear waves [1], fractional Kelvin–Voigt models [2], nonlinear acoustic wave equations [3], fractional Gross–Pitaevskii equations [4], fractional convection-diffusion equations [5], time-fractional Klein–Gordon equations [6], coupled nonlinear Schrödinger equations [7], and anisotropic nonlocal nonlinear fractional Schrödinger equations [8].

These equations have been used to model diverse phenomena, such as calcium sparks in cardiac myocytes [9], Bose-Einstein condensation [10], anomalous heat transport [11], and nonlinear spin dynamics in Heisenberg ferromagnets with conformable time-fractional derivatives [12].

Among these, the nonrelativistic fractional Schrödinger equation, which incorporates non-integer order derivatives in space or time, has garnered considerable attention. It has found applications in a wide range of scientific domains, including nuclear probability and flux densities [13], nonlinear optics and quantum dots [14–16], thermodynamics [17], cluster dynamics [10], quantum decoherence [18], superfluidity [19], and parity-time (PT) symmetric systems [20-22]. Additionally, it has been used to describe phenomena such as Anderson localization of light [23], diffraction-free beams [24], and condensed matter systems [25].

In particular, the optical properties governed by the fractional Schrödinger equation have attracted significant

---

interest. Researchers have investigated beam propagation in various structured media, including honeycomb lattices [26], finite-energy and ring Airy beams [27, 28], dual Airy beams [29], optical Bloch oscillations and Zener tunneling [30], and Hermite-Gaussian solitons [31]. Other optical phenomena studied include wave collapse and self-focusing [32], gap and vortex solitons [33, 34], and beam self-splitting [35].

A particularly intriguing quantum mechanical phenomenon, superarrival, occurs during the transmission or reflection of a wave packet interacting with a time-dependent potential barrier. When the barrier's height is dynamically increased or decreased, a time interval may emerge during which the reflection (or transmission) probability exceeds that of a static barrier. This phenomenon implies that the existence of a perturbation in the potential can lead to superarrival occurrence in the system. Despite its fundamental nature, superarrival has received limited attention, with only a few studies addressing it [8, 23, 24, 29, 36-38].

In the study of the superarrival phenomenon within fractional media, triangular potential barriers play a particularly important role due to their influence on electron reflection, transmission, and tunneling [39, 40]. These concepts are key processes in devices such as planner-doped barrier transistors [41] and field emission sources [40]. These barriers help determine current transport limits and enhance tunneling efficiency, especially when optimized with antireflection coatings. Their dual effect, which facilitates quantum processes while introducing potential reflective losses, makes their study essential for the design and optimization of advanced quantum and optoelectronic systems.

Triangular quantum barriers were therefore chosen for this study based on their superior capacity to capture the nuanced dynamics of quantum tunneling in realistic, non-ideal environments. Compared to traditional rectangular barriers, triangular profiles offer significantly higher tunneling rates, up to three times greater in multibarrier configurations [42], and demonstrate excellent consistency between analytical models and numerical solutions [43]. Their geometry also strongly influences resonant tunneling behavior, as the barrier's slope and height directly shape resonant energy levels and transmission characteristics [44]. These barriers are also central to phenomena such as Klein tunneling in graphene [45] and quantum reflection in doped semiconductor devices [46], reinforcing their applicability to nanoscale and high-speed device design. Importantly, the transport features observed in these systems can guide the development of wave-based metamaterials, where engineered potential landscapes, such as effective triangular profiles, are employed to manipulate transmission, delay, and localization. In contrast to the simplicity of rectangular barriers, triangular potentials offer a more realistic and versatile platform for investigating transport phenomena in fractional and nonlinear media, making them especially well-suited for this study.

While prior studies on superarrival have primarily focused on time-dependent rectangular or idealized potential barriers in standard quantum systems, they rarely explore the impact of fractional-order dynamics or nonlinear interactions. Moreover, the role of potential asymmetry, especially in triangular barriers, remains underexamined. This study distinguishes itself by investigating superarrival in a nonlinear, space-fractional regime, using triangular barriers to capture realistic tunneling dynamics and asymmetry effects. By doing so, it reveals new insights into the interplay between nonlocality, nonlinearity, and geometry in quantum transport, which have not been addressed in earlier works.

To solve the fractional Schrödinger equation and explore such phenomena, a variety of analytical and numerical methods have been employed. These include He's semi-inverse method [47], the Adomian decomposition method [48], (G'/G)-expansion [49], Φ6-model expansion [50], Crank–Nicolson Fourier spectral methods [51], linearly implicit conservative schemes [52], finite element methods [53], the homotopy analysis method [54], and split-step techniques [55-58].

The Split-Step Finite Difference (SSFD) method was chosen for this study due to its proven stability and efficiency in solving time-dependent fractional and nonlinear Schrödinger equations [59–61]. This method allows for the effective decoupling of linear and nonlinear terms [62], enabling accurate simulation of complex wave dynamics in media with nonlocal and nonlinear characteristics. Unlike other numerical schemes that may suffer from instability or require intensive computational resources for fractional operators, the SSFD method provides a balanced approach that ensures both numerical accuracy and computational feasibility for a wide range of parameter regimes [63].

In this manuscript, we investigate the superarrival phenomenon of a Gaussian wavepacket in a fractional quantum medium, focusing on its interaction with a triangular potential barrier. By employing the space-fractional Schrödinger equation, we aim to reveal how dynamic perturbations in such barriers affect wavepacket reflection and transmission. This work not only advances the theoretical understanding of superarrival in fractional and nonlinear media but also has direct implications for metamaterial-based wave control. The demonstrated ability to manipulate transmission timing and amplitude through barrier asymmetry, fractional order, and nonlinearity suggests new strategies for designing metamaterials with tunable wave propagation characteristics. For example, photonic or phononic metamaterials can be engineered with graded or triangular-index profiles and nonlinear components to replicate the enhanced transmission and early arrival effects observed here. Such configurations could be employed in applications like ultrafast optical switching, subwavelength signal routing, or programmable delay lines in integrated wave-based devices.

2. Formalism

The fractional Schrödinger equation governing the dynamics in a fractional medium is expressed as follows:

$$i\frac{\partial}{\partial t}\psi(x,t) = \left[-\kappa\frac{\partial^{\alpha}}{\partial|x|^{\alpha}} + \gamma|\psi(x,t)|^2 + V(x)\right]\psi(x,t) \quad (1)$$

where $1 < \alpha \leq 2$ denotes the Lévy index or the order of the fractional derivative, which is defined as:

$$\frac{\partial^\alpha}{\partial |x|^\alpha} \psi(x,t)$$

$$= \frac{1}{2\cos\left(\frac{\alpha\pi}{2}\right)\Gamma(2-\alpha)} \frac{d^2}{dx^2} \int_{-\infty}^{\infty} |-\xi|^{1-\alpha} \psi(\xi,t)d\xi \qquad (2)$$

where Γ is the gamma function.

In this formulation, the term $\gamma|\psi(x,t)|^2$ represents the nonlinear coulomb interaction, with γ representing its strength. The dispersion coefficient $\kappa = \frac{\hbar^2}{2m^*}$ determines the contribution of the kinetic energy. The external potential ($V(x)$) is modeled as a "triangular potential barrier" in the system, given by:

$$V(x) = V_0(-1 + \frac{sx}{a}) \qquad (3)$$

where $0 \le s \le 1$ controls the slope of the potential. The slope of $s = 0$ corresponds to a flat barrier, while $s = 1$ defines a "diagonal barrier". Besides, the width of the potential is assumed to be $2a$, and V_0 represents the height of the potential, indicating its strength.

As the initial condition, a Gaussian wave packet is considered at time $t = 0$:

$$\psi(x, t = 0) = \exp\left[-\frac{(x-x_0)^2}{\sigma} + ikx\right] \qquad (4)$$

where, x_0, σ, and k denote the initial position, spatial width, and wave number of the wave packet, respectively. In order to study the time evolution of the Gaussian wave packet, $\psi(x, t > 0)$, Eq. (1) is solved numerically using the Split-Step Finite Difference (SSFD) method. This numerical scheme, developed for the standard Schrödinger equation [64], has been extended to solve fractional Schrödinger equation [65].

The transmission coefficient of the Gaussian wave packet is computed as:

$$T = \int_{a}^{+\infty} dx \, |\psi(x,t)|^2 \qquad (5)$$

The main purpose of this study is to evaluate the magnitude of the superarrival of a Gaussian wave packet interacting with a triangular potential barrier. The analysis focuses on the influence of parameters including wave packet width σ, fractional order α, nonlinear strength γ, and dispersion coefficient κ, on the superarrival phenomenon. Following the methodology introduced by Bandyopadhyay [66], the time-dependent transmission coefficients for both the perturbed potential, $T_p(t)$, and free propagation, $T_s(t)$, are plotted. The intersection of these curves defines a characteristic time interval $\Delta t = t_c - t_d$, during which the perturbed transmission exceeds the free propagation counterpart.

The integrated transmission within this interval is given by:

$$I_p = \int_{\Delta t} dt \, T_p(t) \qquad (6\text{-}a)$$

$$I_s = \int_{\Delta t} dt \, T_s(t) \qquad (6\text{-}b)$$

The superarrival coefficient η, quantifying the enhancement, is then defined as:

$$\eta = \frac{I_p - I_s}{I_s} \qquad (7)$$

3. Results and Discussion

In this study, we investigated the superarrival phenomenon exhibited by a Gaussian wave packet propagating through a nonlinear fractional medium containing a triangular potential barrier. The time-dependent fractional Schrödinger equation (Eq. (1)) was numerically solved using the Split-Step Finite Difference (SSFD) method to obtain the evaluation of the wave packet. The transmission coefficient was then evaluated as a function of time to quantify the extent of wave packet transmission across the potential barrier. Subsequently, the superarrival magnitude was computed using Eq. (7), and the influence of key physical parameters including the fractional order, nonlinearity strength, dispersion coefficient, wave packet width, initial velocity of the wave packet, and potential symmetry on the superarrival behavior was explored. For computational convenience, the Planck constant ($\hbar$) and the particle mass (m) were set to unity, thereby the system was simplified into a dimensionless framework.

Two distinct configurations were considered. A triangular potential barrier with a fixed height V_0=0.7 and a total width of 2a=100 was employed. In the first scenario, the Gaussian wave packet which is initialized at an appropriate distance from the barrier, propagated toward the sloped side of the potential barrier. In the second scenario, the wave packet approached the flat side of the potential barrier. By comparing the results obtained from these two configurations, the influence of potential symmetry on the superarrival phenomenon was explicitly investigated. To illustrate the schematic representation of the two scenarios discussed above, Figure 1 presents the corresponding configurations.

To explore the effect of the potential gradient, the slope parameter s was varied in 10 discrete steps: $s = 0, 0.1, 0.2, \dots, 1$. For clearer visualization, the resulting superarrival magnitudes were plotted as a function of the $10s$ across all simulations.

At first, preliminary simulations were conducted to examine the impact of varying initial wave packet velocities on the superarrival magnitude. These simulations allowed us to identify an optimal initial velocity at which the superarrival effect was most pronounced. Although the corresponding results are not presented graphically for the sake of conciseness, the analysis led to the selection of a wave packet with an initial velocity $v = 1.5$ for all subsequent simulations. Thereafter, the effects of the dispersion coefficient, nonlinearity strength, Lévy index, and wave packet width on the superarrival phenomenon were compared for the two aforementioned configurations.

Figure 2 presents the superarrival coefficient as a function of the Gaussian wave packet width for the case where the wave packet tunneled through the sloped side of the triangular potential barrier. To isolate the effect of wave packet width on the superarrival magnitude, the dispersion coefficient was fixed at $\kappa = 0.5$, the medium was considered fully fractional with $\alpha = 1.01$, and nonlinearity

was excluded by setting $\gamma = 0$. As shown in Figure 2, the superarrival magnitude increases with increasing wave packet width. Based on this observation, a wave packet with a width of $\sigma = 100$ was selected for subsequent simulations aimed at investigating the influence of other physical parameters on the superarrival phenomenon.
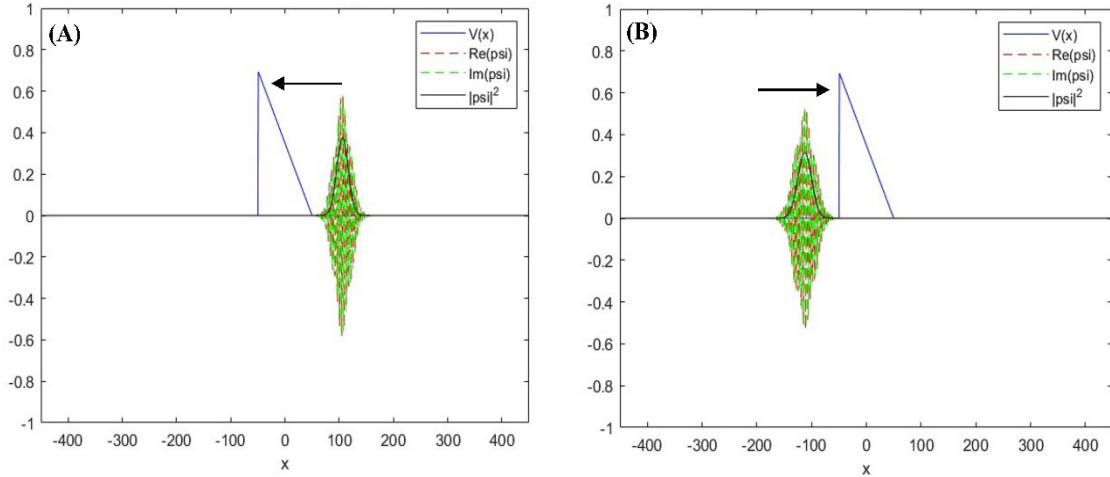

Fig. 1. A schematic illustration of the initial configuration assumed in the simulation. Panel (A) shows a Gaussian wave packet propagating toward the sloped side of the triangular potential barrier. Panel (B) shows the same configuration as in panel (A) but with the wave packet propagating toward the flat side of the potential barrier. In both panels, the arrow indicates the direction of wave packet propagation.

To explore the effect of the potential gradient, the slope parameter s was varied in 10 discrete steps: $s = 0, 0.1, 0.2, \ldots, 1$. For clearer visualization, the resulting superarrival magnitudes were plotted as a function of the $10s$ across all simulations.

At first, preliminary simulations were conducted to examine the impact of varying initial wave packet velocities on the superarrival magnitude. These simulations allowed us to identify an optimal initial velocity at which the superarrival effect was most pronounced. Although the corresponding results are not presented graphically for the sake of conciseness, the analysis led to the selection of a wave packet with an initial velocity $v = 1.5$ for all subsequent simulations. Thereafter, the effects of the dispersion coefficient, nonlinearity strength, Lévy index, and wave packet width on the superarrival phenomenon were compared for the two aforementioned configurations.

Figure 2 presents the superarrival coefficient as a function of the Gaussian wave packet width for the case where the wave packet tunneled through the sloped side of the triangular potential barrier. To isolate the effect of wave packet width on the superarrival magnitude, the dispersion coefficient was fixed at $\kappa = 0.5$, the medium was considered fully fractional with $\alpha = 1.01$, and nonlinearity was excluded by setting $\gamma = 0$. As shown in Figure 2, the superarrival magnitude increases with increasing wave packet width. Based on this observation, a wave packet with a width of $\sigma = 100$ was selected for subsequent simulations aimed at investigating the influence of other physical parameters on the superarrival phenomenon.
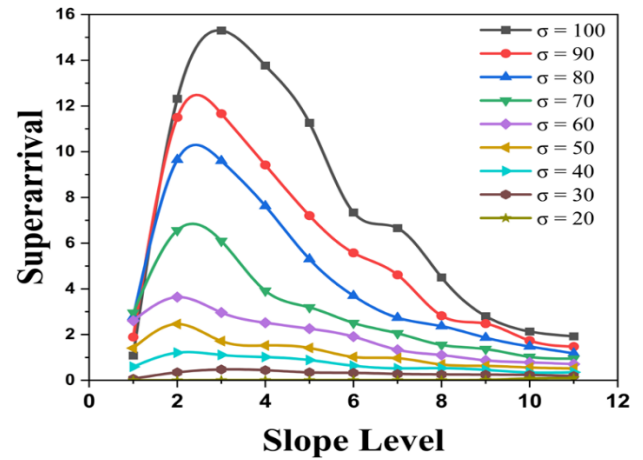

Fig. 2. Superarrival magnitude as a function of the potential slope for wave packets with different widths (σ).

To more clearly illustrate the effect of the dispersion coefficient on the superarrival phenomenon, Figure 3 presents the relevant results. Panel (A) illustrates the variation of the superarrival magnitude as a function of the potential slope parameter for a Gaussian wave packet incident on the sloped side of the potential barrier. Multiple dispersion coefficients are considered that are represented by curves with different colors and symbols. Panel (B) presents the corresponding results for a Gaussian wave packet approaching the flat side of the barrier. In both cases, the medium was assumed to be fully fractional ($\alpha = 1.01$) and linear ($\gamma = 0$).

From panels (A) and (B) of Figure 3, it is evident that both configurations exhibit a similar trend in superarrival

variation with increasing dispersion coefficient. In the system with dispersion coefficient $\kappa = 0.5$, the superarrival curve shows a peak near $s = 0.2$, and then with decreasing the potential slope, the superarrival gradually reduces. Moreover, an increase in the dispersion coefficient results in a monotonic reduction of the superarrival magnitude across the entire slope range. This behavior can be attributed to the fact that a larger dispersion coefficient leads to a faster spatial spreading of the wave packet during propagation. As a result, the wave packet undergoes a broader and more diffuse interaction with the potential barrier, which increases the overall transmission time. Consequently, the coherence required for the emergence of the superarrival effect diminishes, resulting in a decrease in its magnitude. Additionally, a comparison between panels (A) and (B) reveals that, under identical conditions, the superarrival effect is generally more pronounced when the wave packet propagates toward the sloped side of the barrier compared to the flat side. These results suggest that potential asymmetry played a significant role in enhancing the superarrival phenomenon.

As previously discussed, according to Figure 3, for $\kappa > 1.0$, the superarrival exhibits a linear dependence on the potential slope. Therefore, $\kappa = 1.0$ was fixed for the remainder of the simulations.
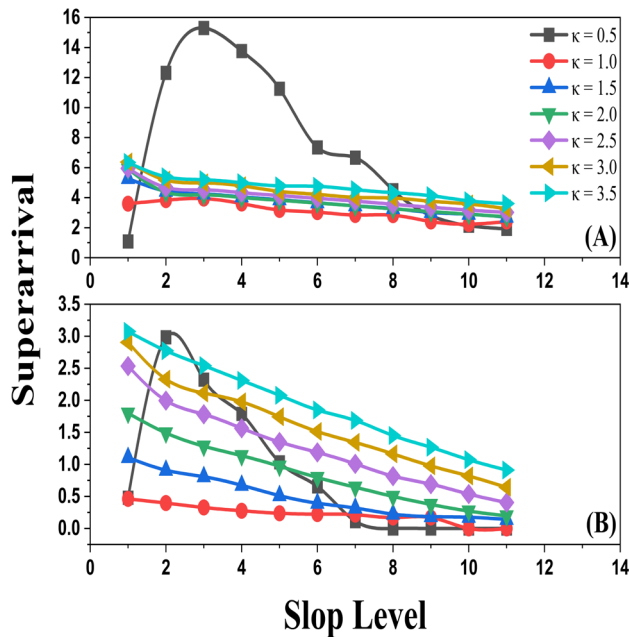
Fig. 3. Superarrival magnitude as a function of the potential slope for media with different dispersion coefficients through which the wave packet propagates. Panel A corresponds to the case in which the wave packet approaches the sloped side of the potential barrier, while panel B is related to the case in which the wave packet approaches the flat side of the potential barrier. In both panels $\alpha = 1.01$ and $\gamma = 0$.

Next, the influence of the fractional parameter α on the superarrival behavior of the wave packet was investigated for the two previously discussed scenarios. Figure 4 illustrates the variation of the superarrival coefficient η as a function of the potential slope. The curves corresponding to different Lévy indices are distinguished by lines with varying colors and symbols. Panel (A) presents the case

where the wave packet traverses the sloped side of the potential, whereas, panel (B) corresponds to the propagation through the flat side.

As shown in Figure 4, for $\gamma = 0$ and $\kappa = 1.0$, a decrease in the Lévy parameter leads to an enhancement of the superarrival effect. Specifically, in the standard Schrödinger regime ($\alpha = 2.0$), the superarrival phenomenon is not observed, whereas, in a fully fractional medium ($\alpha = 1.01$), the superarrival magnitude reaches its maximum value. This behavior can be attributed to the increased localization of the wave packet in fractional systems with smaller Lévy parameters. It allows wave packets to propagate more effectively through the system and facilitate the occurrence of superarrival.

It is also noteworthy that when the wave packet encounters the flat side of the potential barrier in a medium with a fractional coefficient greater than 1.3, the superarrival phenomenon is suppressed. This result further highlights the role of potential symmetry in inhibiting the occurrence of superarrival in the system.
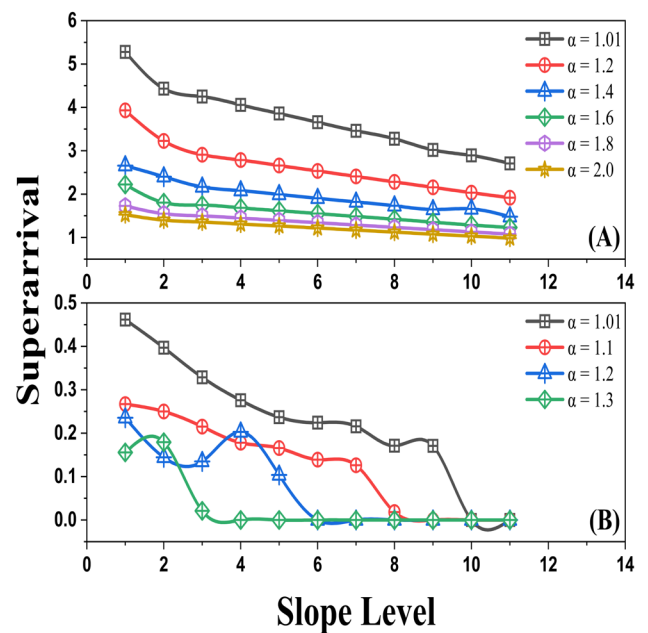
Fig. 4. Superarrival magnitude as a function of the potential slope for media with different fractional orders through which the wave packet propagates. Panel A corresponds to the case in which the wave packet approaches the sloped side of the potential barrier, while panel B is related to the case in which the wave packet approaches the flat side of the potential barrier. In both panels $\kappa = 1$ and $\gamma = 0$.

Here, the effect of system nonlinearity on the superarrival of Gaussian wave packets propagating through the triangular potential barrier was studied. Panel (A) of Figure 5 presents the variation of the superarrival coefficient (η) as a function of the potential slope parameter (s) for a wave packet incident on the sloped side of the potential, under different nonlinearity strengths.

Panel (B) displays analogous results for a wave packet incident on the flat side of the potential barrier. Curves corresponding to different nonlinear coefficients (γ) are distinguished by varying colors and symbols.
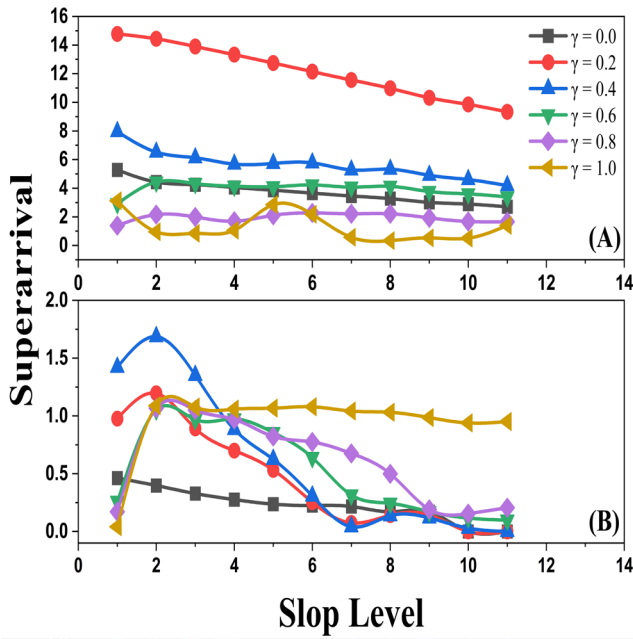
Fig. 5. Superarrival magnitude as a function of the potential slope for media with different nonlinearity through which the wave packet propagates. Panel A corresponds to the case in which the wave packet approaches the sloped side of the potential barrier, while panel B is related to the case in which the wave packet approaches the flat side of the potential barrier. In both panels $\alpha = 1.01$ and $\kappa = 1$.

As observed, the superarrival magnitude exhibits fluctuations as the nonlinearity of the system changes. A comparison between panels (A) and (B) reveals that superarrival associated with wave packets encountering the sloped side of the potential is generally more pronounced than that observed for those encountering the flat side. Specifically, in the linear regime ($\gamma = 0$), the superarrival for a completely flat potential ($s = 0$) is approximately 5 and decreases linearly to about 4 as the slope parameter increases. When the nonlinearity parameter increases to $\gamma = 0.2$, the superarrival magnitude rises sharply to approximately 15, before decreasing to around 10 as the slope increases. As the nonlinearity strength continues to increase beyond this point, η gradually decreases and eventually vanishes.

For a wave packet incident on the flat side of the potential barrier, the superarrival similarly fluctuates with increasing nonlinearity, although with lower overall magnitudes compared to the sloped side case. Consistent with the observations in Figure 4, Figure 5 clearly demonstrates that the symmetry of the potential can suppress the superarrival phenomenon. It is also noteworthy that, in this case, the maximum superarrival magnitude is observed for a system with a nonlinear coefficient around $\gamma = 0.4$.

4. Conclusions

In this study, a detailed investigation into the superarrival phenomenon exhibited by Gaussian wave packets propagating through a nonlinear fractional medium characterized by a triangular potential barrier has

been conducted. By numerically solving the time-dependent fractional Schrödinger equation using the Split-Step Finite Difference (SSFD) method, the transmission dynamics have been examined and the superarrival magnitude under varying physical conditions and configurations has been evaluated.

The results reveal that the superarrival effect is highly sensitive to several key system parameters, including the fractional order of the medium, the nonlinearity strength, the dispersion coefficient, the wave packet width, and the initial velocity of the wave packet. Furthermore, the symmetry and slope of the potential barrier were found to significantly influence the occurrence of superarrival. Specifically, asymmetry in the potential, introduced through a sloped barrier, was shown to enhance the superarrival effect, whereas symmetry, represented by the flat side, tended to suppress it.

An increase in the wave packet width led to a more pronounced superarrival effect, suggesting that broader wave packets maintain coherence more effectively during propagation. Conversely, higher dispersion coefficients reduced the magnitude of superarrival, which is attributed to the rapid spatial spreading of the wave packet that diminishes coherence and increases transmission time. The fractional nature of the medium, quantified by the Lévy index, also played a critical role.

A decrease in the Lévy parameter, corresponding to a more fractional regime, enhanced the superarrival effect due to increased localization and more efficient propagation dynamics. Notably, in the standard quantum mechanical regime ($\alpha = 2.0$), the superarrival phenomenon was not observed, highlighting the unique contributions of fractional dynamics.

The presence of nonlinearity introduced a non-monotonic dependence in the superarrival behavior. A moderate level of nonlinearity significantly enhances the superarrival magnitude, whereas further increases lead to its gradual suppression. This behavior indicates the existence of an optimal nonlinear regime in which superarrival is maximized. Additionally, comparisons between scenarios where the wave packet. Furthermore, the symmetry and slope of the potential barrier were found to significantly influence the occurrence of superarrival. Specifically, asymmetry in the potential, introduced through a sloped barrier, was shown to enhance the superarrival effect, whereas symmetry, represented by the flat side, tended to suppress it.

An increase in the wave packet width led to a more pronounced superarrival effect, suggesting that broader wave packets maintain coherence more effectively during propagation. Conversely, higher dispersion coefficients reduced the magnitude of superarrival, which is attributed to the rapid spatial spreading of the wave packet that diminishes coherence and increases transmission time.

The fractional nature of the medium, quantified by the Lévy index, also played a critical role. A decrease in the Lévy parameter, corresponding to a more fractional regime, enhanced the superarrival effect due to increased localization and more efficient propagation dynamics. Notably, in the standard quantum mechanical regime (α = 2.0), the superarrival phenomenon was not observed, highlighting the unique contributions of fractional dynamics.

The presence of nonlinearity introduced a non-monotonic dependence in the superarrival behavior. A moderate level of nonlinearity significantly enhances the superarrival magnitude, whereas further increases lead to its gradual suppression. This behavior indicates the existence of an optimal nonlinear regime in which superarrival is maximized. Additionally, comparisons between scenarios where the wave packet encountered the sloped versus the flat side of the potential barrier consistently showed that the superarrival magnitude was greater in the asymmetric (sloped) case, underscoring the critical influence of potential symmetry on the effect.

Overall, the findings of this study provide valuable insights into the interplay between fractional dynamics, nonlinearity, and potential asymmetry in governing early transmission phenomena in quantum systems. These results contribute to a deeper theoretical understanding of superarrival and may inform future investigations into quantum control, wave packet engineering, and transport phenomena in complex media.

Funding Statement

Conflicts of interest

Professor Mohammad Hossein Ehsani, the corresponding author of this paper is the current Director-in-Charge of Progress in Physics of Applied Materials (PPAM), but he has no involvement in the peer review process used to assess this work submitted to the Journal. This paper was assessed, and the corresponding peer review managed by Dr. Sanaz Alamdari, the Executive Manager of PPAM.

Authors contribution statement

Methodology: (M.S., M.S.)
Formal analysis: (M.S.)
Investigation: (M.S.)
Data curation: (M.S.)
Writing-original draft: (M.S.)
Supervision: (M.H.E)
Writing-review and editing: (M.H.E., M.S.)

References

[1] Holm, Sverre, and Ralph Sinkus. "A unifying fractional wave equation for compressional and shear waves." *The Journal of the Acoustical Society of America* 127.1 (2010): 542-548.

[2] Holm, Sverre, and Sven Peter Näsholm. "A causal and fractional all-frequency wave equation for lossy media." *The Journal of the Acoustical Society of America* 130.4 (2011): 2195-2202.

[3] Prieur, Fabrice, Gregory Vilenskiy, and Sverre Holm. "A more fundamental approach to the derivation of nonlinear acoustic wave equations with fractional loss operators (L)." *The Journal of the Acoustical Society of America* 132.4 (2012): 2169-2172.

[4] Uzar, Neslihan, and Sedat Ballikaya. "Investigation of classical and fractional Bose–Einstein condensation for harmonic potential." *Physica A: Statistical Mechanics and its Applications* 392.8 (2013): 1733-1741.

[5] Merdan, M. "Analytical approximate solutions of fractionel convection-diffusion equation with modified Riemann-Liouville derivative by means of fractional variational iteration method." *Iranian Journal of Science* 37.1 (2013): 83-92.

[6] Hosseini, Kamyar, Peyman Mayeli, and Reza Ansari. "Bright and singular soliton solutions of the conformable time-fractional Klein–Gordon equations with different nonlinearities." *Waves in Random and Complex Media* 28.3 (2018): 426-434.

[7] Zhang, Jinggui. "Modulation instability of copropagating optical beams in fractional coupled nonlinear schrödinger equations." *Journal of the Physical Society of Japan* 87.6 (2018): 064401.

[8] Wang, Qing, and ZhenZhou Deng. "Elliptic solitons in (1+ 2)-dimensional anisotropic nonlocal nonlinear fractional Schrödinger equation." *IEEE Photonics Journal* 11.4 (2019): 1-8.

[9] Tan, Wenchang, et al. "An anomalous subdiffusion model for calcium spark in cardiac myocytes." *Applied physics letters* 91.18 (2007).

[10] Herrmann, Richard. "Fractional phase transition in medium size metal clusters." *Physica A: Statistical Mechanics and its Applications* 389.16 (2010): 3307-3315.

[11] Buonocore, Salvatore, and Fabio Semperlotti. "Tomographic imaging of non-local media based on space-fractional diffusion models." *Journal of Applied Physics* 123.21 (2018).

[12] Hashemi, M. S. "Some new exact solutions of (2+ 1)-dimensional nonlinear Heisenberg ferromagnetic spin chain with the conformable time fractional derivative." *Optical and Quantum Electronics* 50.2 (2018): 79.

[13] Medina, Leidy Y., Francisco Núñez-Zarur, and Jhon F. Pérez-Torres. "Nonadiabatic effects in the nuclear probability and flux densities through the fractional Schrödinger equation." *International Journal of Quantum Chemistry* 119.16 (2019): e25952.

[14] Dawson, Nathan J., Onassis Nottage, and Moussa Kounta. "The second hyperpolarizability of systems described by the space-fractional Schrödinger equation." *Physics Letters A* 382.1 (2018): 55-59.

[15] Hasan, Mohammad, and Bhabani Prasad Mandal. "Tunneling time in space fractional quantum mechanics." *Physics Letters A* 382.5 (2018): 248-252.

[16] El-Nabulsi, Rami Ahmad. "Time-fractional Schrödinger equation from path integral and its implications in

quantum dots and semiconductors." *The European Physical Journal Plus* 133.10 (2018): 394.

[17] Mondol, Adreja, et al. "An insight into Newton's cooling law using fractional calculus." *Journal of Applied Physics* 123.6 (2018).

[18] Kirkpatrick, Kay, and Yanzhi Zhang. "Fractional Schrödinger dynamics and decoherence." *Physica D: Nonlinear Phenomena* 332 (2016): 41-54.

[19] Tayurskii, D. A., and Yu V. Lysogorskiy. "Superfluid hydrodynamic in fractal dimension space." *Journal of Physics: Conference Series*. Vol. 394. No. 1. IOP Publishing, 2012.

[20] Yao, Xiankun, and Xueming Liu. "Solitons in the fractional Schrödinger equation with parity-time-symmetric lattice potential." *Photonics Research* 6.9 (2018): 875-879.

[21] Li, Pengfei, et al. "PT-symmetric optical modes and spontaneous symmetry breaking in the space-fractional Schrödinger equation." *Rom. Rep. Phys* 71.2 (2019): 106.

[22] Zhan, Kaiyun, et al. "Defect modes of defective parity-time symmetric potentials in one-dimensional fractional Schrödinger equation." IEEE Photonics Journal 9.6 (2017): 1-8.

[23] Huang, Changming, et al. "Localization and Anderson delocalization of light in fractional dimensions with a quasi-periodic lattice." Optics Express 27.5 (2019): 6259-6267.

[24] Zhang, Y., et al. "Diffraction free beams in fractional Schrödinger equation, Sci." Rep. (UK) 6 (2016): 1-8.

[25] Stickler, B. A. "Potential condensed-matter realization of space-fractional quantum mechanics: The one-dimensional Lévy crystal." Physical Review E—Statistical, Nonlinear, and Soft Matter Physics 88.1 (2013): 012120.

[26] Zhang, Da, et al. "Unveiling the link between fractional Schrödinger equation and light propagation in honeycomb lattice." Annalen der Physik 529.9 (2017): 1700149.

[27] Huang, Xianwei, Zhixiang Deng, and Xiquan Fu. "Dynamics of finite energy Airy beams modeled by the fractional Schrödinger equation with a linear potential." Journal of the Optical Society of America B 34.5 (2017): 976-982.

[28] Huang, Xianwei, et al. "Propagation characteristics of ring Airy beams modeled by fractional Schrödinger equation." Journal of the Optical Society of America B 34.10 (2017): 2190-2197.

[29] Zang, Feng, Yan Wang, and Lu Li. "Self-induced periodic interfering behavior of dual Airy beam in strongly nonlocal medium." Optics Express 27.10 (2019): 15079-15090.

[30] Zhang, Yiqi, et al. "Optical Bloch oscillation and Zener tunneling in the fractional Schrödinger equation." Scientific Reports 7.1 (2017): 17872.

[31] Wang, Qing, et al. "Hermite-gaussian–like soliton in the nonlocal nonlinear fractional Schrödinger equation." Europhysics Letters 122.6 (2018): 64001.

[32] Chen, Manna, et al. "Optical solitons, self-focusing, and wave collapse in a space-fractional Schrödinger equation with a Kerr-type nonlinearity." Physical Review E 98.2 (2018): 022211.

[33] Huang, Changming, et al. "Gap solitons in fractional dimensions with a quasi-periodic lattice." Annalen der Physik 531.9 (2019): 1900056.

[34] Yao, Xiankun, and Xueming Liu. "Off-site and on-site vortex solitons in space-fractional photonic lattices." Optics Letters 43.23 (2018): 5749-5752.

[35] Meng, Yunji, et al. "Self-splitting of spatial solitons in a nonlinear fractional Schrödinger equation with a longitudinal potential barrier." Optics Communications 440 (2019): 68-74.

[36] Zhang, Lifu, et al. "Propagation dynamics of super-Gaussian beams in fractional Schrödinger equation: from linear to nonlinear regimes." Optics express 24.13 (2016): 14406-14418.

[37] Dong, Liangwei, and Changming Huang. "Double-hump solitons in fractional dimensions with a $\mathcal{PT}$–symmetric potential." Optics Express 26.8 (2018): 10509-10518.

[37] Dong, Liangwei, and Changming Huang. "Double-hump solitons in fractional dimensions with a $\mathcal{PT}$–symmetric potential." Optics Express 26.8 (2018): 10509-10518.

[38] Amadou, Yaouba, et al. "Fractional effects on solitons in a 1D array of rectangular ferroelectric nanoparticles." Waves in Random and Complex Media 30.3 (2020): 581-592.

[39] Forbes, Richard G., and Jonathan HB Deane. "Transmission coefficients for the exact triangular barrier: an exact general analytical theory that can replace Fowler & Nordheim's 1928 theory." Proceedings of the Royal Society A: Mathematical, Physical and Engineering Sciences 467.2134 (2011): 2927-2947.

[40] Zhao, Zijun C., and David R. McKenzie. "Antireflection coating of barriers to enhance electron tunnelling: exploring the matter wave analogy of superluminal optical phase velocity." Scientific reports 7.1 (2017): 12772.

[41] Chandra, Amitabh, and Lester F. Eastman. "Quantum mechanical reflection at triangular``planar-doped''potential barriers for transistors." Journal of Applied Physics 53.12 (1982): 9165-9169.

[42] Leite, Telio Nobre, and Helinando Pequeno de Oliveira. "Tunneling processes in a triangular multibarrier semiconductor heterostructure." IEEE transactions on electron devices 58.3 (2011): 716-719.

[43] Mahajan, Ashutosh, and Swaroop Ganguly. "An analytical model for electron tunneling in triangular quantum wells." Semiconductor Science and Technology 36.5 (2021): 055012.

[44] Ohmukai, Masato. "Triangular double barrier resonant tunneling." Materials Science and Engineering: B 116.1 (2005): 87-90.

[45] Mekkaoui, Miloud, Ahmed Jellal, and Hocine Bahlouli. "Tunneling of electrons in graphene via double triangular barrier in external fields." Solid State Communications 358 (2022): 114981.

[46] Chandra, Amitabh, and Lester F. Eastman. "Quantum mechanical reflection at triangular``planar doped ''potential barriers for transistors." Journal of Applied Physics 53.12 (1982): 9165-9169.

[47] Wang, Gangwei, and Tianzhou Xu. "Optical soliton of time fractional Schrödinger equations with He's semi-inverse method." Laser Physics 25.5 (2015): 055402.

[48] Rida, S. Z., H. M. El-Sherbiny, and A. A. M. Arafa. "On the solution of the fractional nonlinear Schrödinger equation." Physics Letters A 372.5 (2008): 553-558.

[49] Khater, Mostafa MA, Aly R. Seadawy, and Dianchen Lu. "New optical soliton solutions for nonlinear complex fractional Schrödinger equation via new auxiliary equation method and novel (G′/G) (G′/G)-expansion method." Pramana 90 (2018): 1-20.

[50] Zayed, Elsayed ME, and Abdul-Ghani Al-Nowehy. "The ϕ 6-model expansion method for solving the nonlinear conformable time-fractional Schrödinger equation with fourth-order dispersion and parabolic law nonlinearity." Optical and Quantum Electronics 50.3 (2018): 164.

[51] Zhang, Hui, et al. "Crank–Nicolson Fourier spectral methods for the space fractional nonlinear Schrödinger equation and its parameter estimation." International Journal of Computer Mathematics 96.2 (2019): 238-263.

[52] Wang, Dongling, Aiguo Xiao, and Wei Yang. "A linearly implicit conservative difference scheme for the space fractional coupled nonlinear Schrödinger equations." *Journal of Computational Physics* 272 (2014): 644-655.

[53] Li, Meng, et al. "A fast linearized conservative finite element method for the strongly coupled nonlinear fractional Schrödinger equations." *Journal of Computational Physics* 358 (2018): 256-282.

[54] Khan, Najeeb Alam, Muhammad Jamil, and Asmat Ara. "Approximate solutions to time-fractional Schrödinger equation via homotopy analysis method." *International Scholarly Research Notices* 2012.1 (2012): 197068.

[55] Wang, Pengde, and Chengming Huang. "Split-step alternating direction implicit difference scheme for the fractional Schrödinger equation in two dimensions." *Computers & Mathematics with Applications* 71.5 (2016): 1114-1128.

[56] Zhang, Yiqi, et al. "Optical Bloch oscillation and Zener tunneling in the fractional Schrödinger equation." *Scientific Reports* 7.1 (2017): 17872.

[57] Hasan, Mohammad, and Bhabani Prasad Mandal. "Tunneling time in space fractional quantum mechanics." *Physics Letters A* 382.5 (2018): 248-252.

[58] Li, Meng. "A high-order split-step finite difference method for the system of the space fractional CNLS." *The European Physical Journal Plus* 134.5 (2019): 244.

[59] Solaimani, M. "Nontrivial wave-packet collision and broadening in fractional Schrodinger equation formalism." *Journal of Modern Optics* 67.12 (2020): 1128-1137.

[60] Farag, Neveen GA, et al. "Numerical Solutions of the (2+ 1)-Dimensional Nonlinear and Linear Time-Dependent Schrödinger Equations Using Three Efficient Approximate Schemes." *Fractal and Fractional* 7.2 (2023): 188.

[61] Li, Meng. "A high-order split-step finite difference method for the system of the space fractional CNLS." *The European Physical Journal Plus* 134.5 (2019): 244.

[62] Nizam, Elminur, and Kaysar Rahman. "A Compact Split-step Finite Difference Method for Solving the Nonlinear Schrödinger Equation." *Journal of Physics: Conference Series*. Vol. 2660. No. 1. IOP Publishing, 2023.

[63] Zhu, Pengfei, Lan Wang, and Qiang Li. "High order compact split step finite difference method for two-dimensional coupled nonlinear Schrödinger system." *Journal of Physics: Conference Series*. Vol. 2202. No. 1. IOP Publishing, 2022.

[64] Vatan, M., et al. "Transport properties of a traveling wave packet through rectangular quantum wells and barriers." *Optik* 136 (2017): 281-288.

[65] Solaimani, M. "Nontrivial wave-packet collision and broadening in fractional Schrodinger equation formalism." *Journal of Modern Optics* 67.12 (2020): 1128-1137.

[66] Bandyopadhyay, Somshubhro, A. S. Majumdar, and Dipankar Home. "Quantum-mechanical effects in a time-varying reflection barrier." *Physical Review A* 65.5 (2002): 052718.